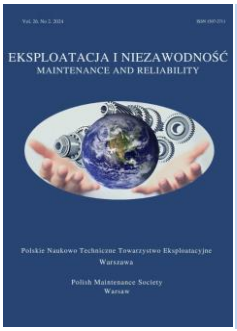

Eksploatacja i Niezawodnosc – Maintenance and Reliability

Volume 26 (2024), Issue 2

journal homepage: http://www.ein.org.pl

Article citation info:
Wieczorek A. N, Konieczny L, Wojnar G, Wyroba R, Filipowicz K, Kuczaj M, Reduction of dynamic loads in the drive system of mining scraper conveyors through the use of an innovative highly flexible metal coupling, Eksploatacja i Niezawodnosc – Maintenance and Reliability 2024: 26(2) http://doi.org/10.17531/ein/181171

Reduction of dynamic loads in the drive system of mining scraper conveyors through the use of an innovative highly flexible metal coupling

Indexed by: Web of Science Group

Andrzej Norbert Wieczorek[a,*], Łukasz Konieczny[a], Grzegorz Wojnar[a], Rafał Wyroba[b], Krzysztof Filipowicz[a], Mariusz Kuczaj[a]

[a] Silesian Technical University, Poland
[b] Patentus SA, Poland

Highlights

- The paper discusses studies of a power transmission system featuring a torsionally flexible metal clutch of innovative design, transferring a high torque, which is considered a novelty given the current state of technology.
- The experiments conducted under the studies revealed that the gear transmission vibrations had been successfully reduced, which should be attributed to the resulting reduction of the dynamic forces triggered by external factors.
- Following tests conducted in operating conditions, the highly flexible clutches of innovative design were found to be suitable for mining conveyors operating under high loads.

Abstract

The article provides a discussion on the results of the authors' original studies of a power transmission system of a mining scraper conveyor coupled with an innovative highly flexible clutch, conducted in operating conditions. The research consisted in establishing the static characteristics of the highly flexible clutch in question, determining the torsional vibrations of the said highly flexible clutch and the vibrations of the transmission housings at a test rig, verifying if the coupling between the innovative flexible clutch and a typical scraper conveyor drive unit was correct, and testing durability of individual components of the highly flexible clutch. Following the aforementioned tests and based on the static characteristics of the highly flexible clutch examined, one can distinguish three phases of its operation: initial, main, and final – all differing in terms of flexibility. Furthermore, upon increasing the flexibility of the metal clutch, a significant decline in the root mean square (RMS) values of linear vibration accelerations was observed compared to the blocked condition of the clutch. It was further noticed that, as the torsional vibrations of the clutch shaft were increasing, the linear vibrations measured at the transmission bearing housings were decreasing significantly. Based on the tests conducted in operating conditions, it was found that the durability of the flexibilising system (bolt and nut) was sufficient and that there were no thermal effects associated with the motion of the system components.

Keywords
gears, conveyors, torsionally flexible metal clutch, vibrations, reduction

1. Introduction

Longwall scraper conveyors (Fig. 1) are machines [57] functioning as sub-assemblies of powered hard coal mining systems, and therefore, the total cost-effectiveness of mines depends on how durable they are.

A typical drive system of a scraper conveyor [27, 51] consists of an asynchronous motor, a flexible and/or hydrokinetic clutch, a gear transmission, and a chain drum [60, 70]. Such elements of this system as gear teeth, bearings, chains,

(*) Corresponding author.
E-mail addresses: A. N. Wieczorek (ORCID: 0000-0002-8634-7763) andrzej.n.wieczorek@polsl.pl, L. Konieczny (ORCID: 0000-0002-9501-7651) lukasz.konieczny@polsl.pl, G. Wojnar (ORCID: 0000-0003-3515-3990) grzegorz.wojnar@polsl.pl, R. Wyroba, r.wyroba@patentus.pl, K. Filipowicz (ORCID: 0000-0001-6672-1378) krzysztof.filipowicz@polsl.pl, M. Kuczaj (ORCID: 0000-0001-6893-0309) mariusz.kuczaj@polsl.pl.

and chain drums are heavily exposed to certain environmental factors in the course of their operation [60, 63, 69]. Their defects are most frequently caused by tribological [72] factors (this problem has been discussed extensively in numerous publications, including [18, 61]), but also by the impact of dynamic forces, the latter being the subject of this paper. In scraper conveyors, one of the characteristics of the operation process is that dynamic loads [67], occur not only at the start-up, but also during regular operation [15, 16].

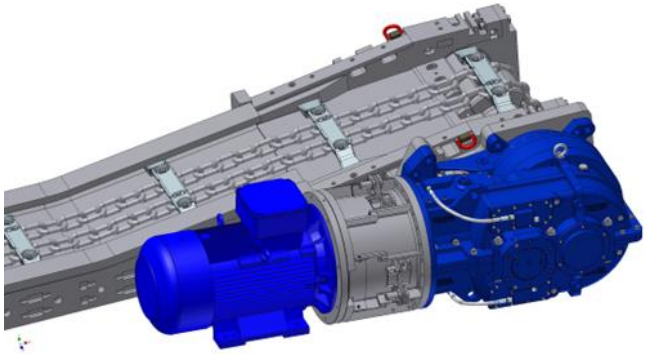

Fig. 1. Drive part of longwall scraper conveyor (source: authors' contribution).

The methods currently applied to increase the service life of the gear transmissions installed in mining conveyor drive systems include using materials of increased wear resistance, predicting technical conditions, and reducing the variability of the load which affects the drive system components [35]. The foregoing pertains particularly to the gear transmissions on which the availability of scraper conveyors depends to the greatest extent.

One can currently observe very intensive development of surface treatment engineering [50] and nanotechnology [53, 58] aimed at improving the durability of superficial layers of materials. Some examples of the state-of-the-art solutions which represent these areas can be found in papers [6, 59]. However, on account of the subject matter of this paper, this problem has not been discussed in more detail.

Great importance has recently been attached to establishing both the reasons for degradation of technical systems and the expected service life, and therefore, advanced data processing methods, including machine learning, are used in these fields.

Angeles and Kumral [1] proposed a new approach to maintenance management that can be applied to the mining industry to improve equipment availability and reliability while preventing potential failures. The issue of reliability of machine systems was analyzed by Michej et al. [42]. A method for analyzing wear particles of gear pump components was presented by Dhote and Khond [12].

Cheng et al. proposed in the article [7] a deep learning-based method called Q-network calibrated ensemble (QCE) for the diagnosis of gears for pumps in the nuclear industry. Dao presented a wind turbine monitoring model based on cointegration in [11].

In turn, Clarke et al [8] compared ultrasonic load measurements on the bearing of a high-speed shaft of a wind turbine gearbox with the results of a static multi-object simulation and found that the measurements made under established operating conditions agreed well with the adopted model. Feng et al. [19, 20] developed a cyclostationary pitting monitoring indicator that can accurately assess the degradation status of the system. Lazarz et al also described in [40] a method for detecting gear damage in the initial phase. New methods of gear monitoring were also presented by Gao et al [23], Gauder [24], Inturi et al. [30], Li et al. [38].

Having acquired such knowledge, one can remedy or reduce the wear of the components of these systems to extend their service life. Moreover, understanding how machines and their components are operated and handled makes it possible to compare diagnostic methods and to predict malfunctions, defects, and failures. The authors of this publication have already referred to some of their experiences in this sphere in their respective papers. For research purposes, vibrations of the driving gear housing were measured in an idling scraper conveyor. The main outcomes of this research included determining the frequencies characteristic of the gear transmission examined and demonstrating the possibility of assessing the technical condition of the gear transmission under conditions of a considerable impact of the conveyor chain. Wieczorek [66], on the other hand, has demonstrated a solution for installing a vibroacoustic and thermal diagnostic system, meeting the relevant ATEX requirements, inside a gear transmission housing, by means of which one could also measure vibrations of scraper conveyor bearings (Fig. 2).

There are at least several ways to limit the impact of dynamic forces acting in gear meshing [50]. One of the most popular methods consists in reducing the value of gear tooth workmanship deviations [37, 68], however, manufacturers have

reached a certain level of gear quality [47] which would be virtually impossible to exceed at this point (4÷6, manufacturing accuracy class as per PN-ISO 1328). A good method to minimise dynamic excitations, also connected with the gear manufacturing phase, is to apply various types of gear tooth modifications [5], however, the effectiveness of this measure is limited to certain constant load values.

Fig. 2. Planetary gear transmission with an ATEX-compliant technical diagnostic system installed inside the housing while in testing (source: authors' contribution).

Another solution used to reduce the vibroactivity of gear transmissions is increasing the workmanship precision of transmission housings [2], particularly with regard to shaft alignment. Based on an analysis of the results obtained in experimental tests, Juzek [31] concluded that misalignment of the transmission shaft axles and its change in the course of tests exerts a significant impact on level of vibrations recorded on the transmission components. In that case, depending on the position of the fixed axle bearing, the differences in the RMS values of vibration signals reached up to several dozen per cent. Nevertheless, the applicability of this solution is limited by the rigidity and accuracy of the machining centres in use.

Another way to reduce the forces acting in the meshing [26] is by avoiding transmission operation in the sub-harmonic or super-harmonic range of resonance, but this requires costly examinations at dedicated test rigs [41] or complex numerical simulations. Increasing the viscosity of the lubricating oil can also result in reduced inter-tooth forces on account of increased damping of the forces acting in gear meshing [25], but at the same time, this increases the hydraulic losses [4, 13] in the gear transmission related to the oil mixing [45, 46] and forcing through in inter-tooth spaces [55, 62].

What can also contribute considerably to the reduction of the dynamic forces observed in the gear meshing [14, 28, 39] is compensating the fluctuations in the meshing rigidity waveform using tall gear teeth, however, at the same time, this triggers an increase in the lubricating oil temperature, and consequently also reduced viscosity [48, 49] and increased power loss in the meshing [64].

Besides minimising the internal forces acting in the gear meshing, one can also reduce the external forces caused by the variability in the process of machinery operation (an example of the behaviour of instantaneous values of the torque loading the drive unit of a scraper conveyor [54] has been shown in Fig. 3). This manner of reducing destructive forces is considered to be particularly important for maintaining the required availability of drive systems, as it can ensure protection against sudden and critical damage to their components. One typically uses mechanical clutches which are optimised against specific operating conditions, and the functions of these clutches include – besides coupling – reducing the forces at play in the system comprising a drive motor, a gear transmission, and a process machine. The available design solutions for chain conveyor drive systems typically include flexible insert-type or – less common – hydrokinetic clutches.

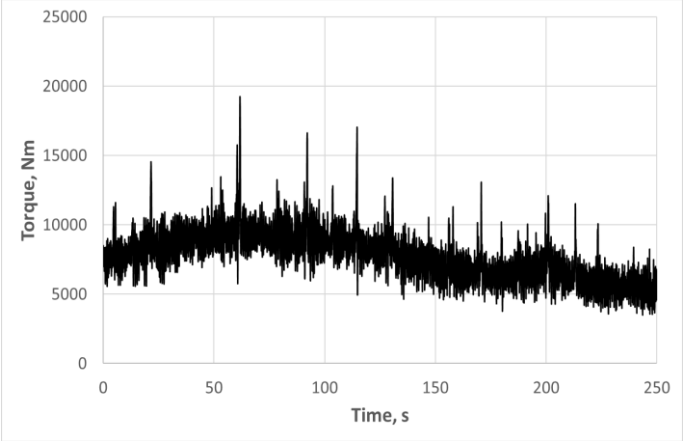

Fig. 3. Example of the behaviour of instantaneous values of torque loading the drive unit of a scraper conveyor, based on [54].

The flexible insert-type clutches represent a very wide and diverse group of devices. The inserts of these clutches are made of rubber or plastic, and they are set between the outline surfaces of discs. These clutches make it possible to transfer a maximum torque of up to 15 kNm. The shape of the working surfaces of the hub jaw and the flexible insert enables the clutch to operate even though the motor shafts and the process device

may be aligned inaccurately [44]. In terms of the limitations of flexible insert clutches, one should particularly mention their small torsion angle and the related inconsiderable reduction of the dynamic forces occurring at start-up and on load changes.

Hydrokinetic clutches are power transmission assemblies where the torque from the active member (pump rotor) is transmitted to the turbine rotor by means of a liquid [22]. The advantages of these clutches include a very soft machine start-up phase, however, they also struggle with significant limitations, such as the following [56, 57]:

- high sensitivity to the liquid level,
- sensitivity to the longitudinal and transverse inclination of drive systems,
- reduction of the nominal power at the turbine shaft by some per cent of its slip relative to the power of the asynchronous engine.

A different approach to reducing dynamic torques in the power transmission system, aimed at extending its service life, has been proposed in papers [26, 29], discussing the use of flexible clutches with adjustable rigidity characteristics. In that case, the rigidity change has been attained by modifying the gas pressure in the pneumatic bellows of this clutch, however, clutches of this type are not suitable for the operating conditions typical of mining conveyors due to their sensitivity to mechanical damage. Another known alternative is a multi-plate clutch of the CST type [17], characterised by adjustable torsional flexibility, but in practice, complex control systems are required to use them for industrial applications, which is why they have not become popular in the mining sector. Some other coupling solutions successfully applied in other industries [9, 10, 26, 52, 71] are simply not suited for the harsh conditions of mining operations, being incapable of transferring the range of loads typical of this sector.

The subject of this paper is the overall body of problems related to the characteristics of vibration and the operational properties of a new solution of a highly flexible metal clutch based on a flexibilising system comprising a bolt and a nut, including a spring pack (the exact structure of the clutch is presented in the work [43]). The design of the innovative clutch (Fig. 4) and its operating principle have been discussed in the papers by Kowal and Filipowicz [32, 33, 34]. This concept has been extended in terms of its utility value and the potential applications of the clutch in numerous further publications, including by Filipowicz [21] who has referred to laboratory tests to demonstrate the beneficial properties of the new clutch in the event that forces of impulse nature should occur. Wieczorek et al. [65] have shown how useful it is to apply a time-frequency processing method to analyse the vibrations of bearings in flexible clutches. Paper [43], on the other hand, discusses the problem of vibration reduction in cylindrical intersecting axis transmissions operating in laboratory conditions following the application of torsionally flexible metal clutches.

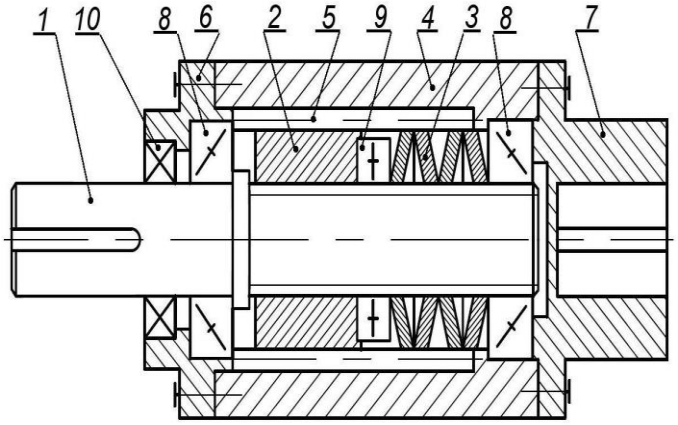

Fig. 4. Torsionally flexible metal clutch; designations: 1 – clutch shaft, 2 – sliding sleeve, 3 – set of disc springs, 4 – clutch housing, 5 – moving splined coupling, 6 – cover, 7 – clutch hub, 8 – cone bearings, 9 – thrust bearing, 10 – sealing ring (based on [34]).

The highly flexible clutch examined under this study was installed in the power transmission system of a longwall scraper conveyor whose gear transmissions were subject to discrete torque excitation. No literature on the subject has yet provided any results of studies on the drive solutions of this kind, which should be regarded as the aspect which makes this paper novel. However, the primary objective of the studies discussed in this article was to verify whether or not the innovative flexible metal clutch in question was suitable for mitigating the effect of dynamically variable load torque on the large-size and high-power multi-stage gear transmissions used in mining scraper conveyors.

2. Research method

For purposes of the studies addressed in this article, a dedicated research method was developed for the new type of clutches discussed, divided into the following 4 stages:

- Stage 1 – determining the static characteristics of the new torsionally flexible clutch under discrete torque excitation conditions; the results thus obtained made it possible to set adequate values of the torque which loaded the power transmission system;
- Stage 2 – determining the torsional vibrations of the flexible clutch and of the transmission housings at a test rig powered by an inverter system enabling the transmission to be loaded with time-varying torque;
- Stage 3 – verifying whether the innovative flexible clutch cooperates correctly with a typical scraper conveyor drive unit based on an assessment of the vibroacoustic effects measured on high-power gear transmission housings;
- Stage 4 – analysing the effect of the elapsed service life of the flexible clutches subject to discrete torque excitation on the vibration reduction efficiency in gear transmission housings and on the surface topography of the components of the clutch being examined.

In order to conduct the tests envisaged under Stages 1÷4, an industrial-class test rig was used, typically serving dynamic acceptance tests of both new and overhauled transmissions with up to 630 kW of power, in accordance with the recommendations provided in the ISO 10816-3 standard. Transmissions are generally tested in a system composed of a power supply inverter, a drive motor, a gear transmission functioning as a reducer, a gear transmission functioning as a multiplier, a motor performing the function of a generator, and an inverter which returns part of the energy to the grid. Such a setup makes it possible to study gear transmissions under load, but energy consumption is only due to friction related losses.

The electric drive unit comprises two Leroy Somer three-phase induction motors with a rated power of 630 kW each. The stators of both machines are supplied power by frequency converters from VACON. This system operates in a closed control loop with feedback provided by a signal received from an encoder installed on the rotor. The inverters communicate with a computer via the MODBUS-TCP protocol. The power supply system allows both motors to be operated in a torque control mode, and the setup also includes a programmable controller which enables the power flow direction to be adjusted in the system during tests without human intervention.

The test rig features a dedicated 16-channel diagnostic system from FAG ProCheck (used to monitor the condition of the clutch and the transmission during the verification tests conducted under Stage 4 of the studies), equipped with acceleration and temperature sensors. The data thus acquired were analysed using the FIS Administrator software. The diagnostic system used in the tests made it possible to monitor data supplied by 16 sensors (8 accelerometers and 8 temperature sensors) mounted on the test transmission and to archive them at the same time. The method of mounting the sensors on the tested devices is presented in [43].

The test object was a flexible clutch (Fig. 5) characterised by a power of 250 kW transmitted at a rotational speed of 1,500 rpm and a safety factor of n=3.

The clutch was attached to the shaft of motor 1 on one side, and on the other side, to a spherical bearing mounted in a bearing housing (Fig. 6). The torque was further transmitted to a reduction gear via a jointed (Cardan) shaft. The gear transmissions (reducer and multiplier) were interconnected by means of a rigid coupling piece, while the multiplier was connected with motor 2 via a Cardan shaft.

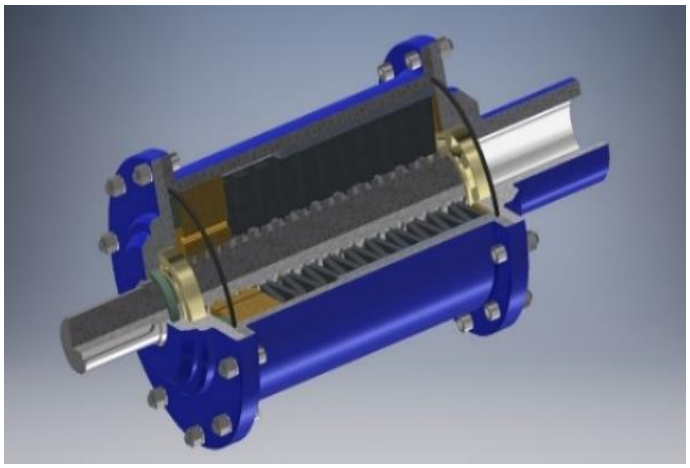

Fig. 5. Highly flexible clutch model (source: authors' contribution).

The manner in which the flexible clutch was mounted on the test rig in Stages 1÷4 was identical. While static, vibroacoustic, and durability characteristics were tested, the gear transmissions were mounted on a special stand which made it possible to

recreate the way in which gear transmissions are installed in scraper conveyors (Fig. 7). Only during the Stage 3 tests, the gear transmissions were mounted in the body of a typical scraper conveyor (Fig. 8).

The static characteristics of the clutch in Stage 1 were established by applying a torque ranging from 100 to 1,400 Nm on the input shaft of the flexible clutch in a single pulse signal of square waveform. This caused torsion of the clutch and stopped it at the position of maximum torsion for a given load, making it possible to read the torsion angle value on a measuring disc (Fig. 9).

Fig. 6. Flexible clutch mounted on the test rig (source: authors' contribution).

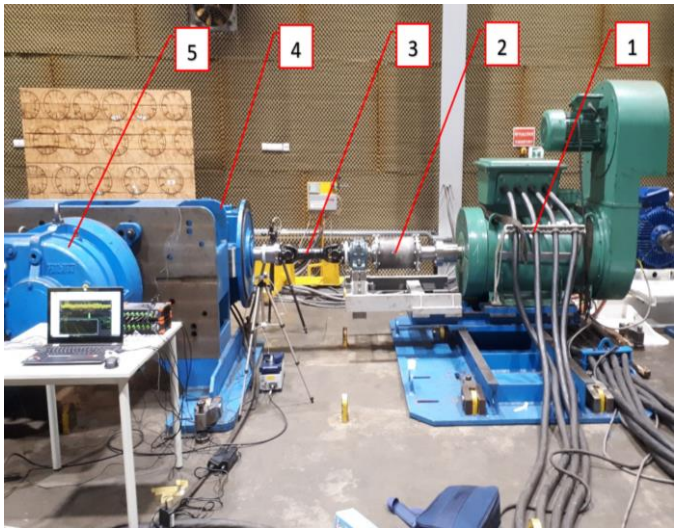

Fig. 7. Gear transmissions mounted on the test rig's stand (Stages 1, 2, and 3); designations: 1 – electric driving motor, 2 – torsionally flexible clutch, 3 – jointed Cardan shaft (3), 4 – stand with 2 gear transmissions (reducer and multiplier), 5 – electric braking motor (source: authors' contribution).

For purposes of the tests envisaged under Stages 2 and 3, an input rotational motor speed oscillating at 1,480 rpm and a square waveform of the braking torque variation were applied during the tests for the following values: 250 ±125 Nm, 500 ±250 Nm, 750 ±375 Nm. Based on previous tests, the load torque variation period was assumed to be 6 seconds. The foregoing represented an attempt to recreate the operation of the conveyor drive system with a momentarily constant load, followed by an abrupt increase in the load due to an abrupt increase in the volume of the load transferred and then an equally abrupt load release once it has been discharged.

Fig.8. Gear transmissions mounted in a scraper conveyor body (source: authors' contribution).

Fig. 9. Measuring disc while determining the static characteristics of the highly flexible clutch (source: authors' contribution).

Under Stage 4, when durability tests were to be performed, it was assumed that more than 1,200 loading cycles would be conducted on the torsionally flexible clutches at a rotational speed of 10 rpm and with a torsional moment of 300 ±290 Nm being applied in a discrete manner at the test rig described above.

A measuring set comprising the Sirius 16-channel data

acquisition card and the Dewesoft software was used to measure vibration signals and to determine the time base, while the RLV-5500 laser vibration meter from Polytec was used for contactless measurements of instantaneous angular velocities of the flexible clutch shaft. A schematic diagram showing the arrangement of the measuring sensors has been provided in Fig. 10.

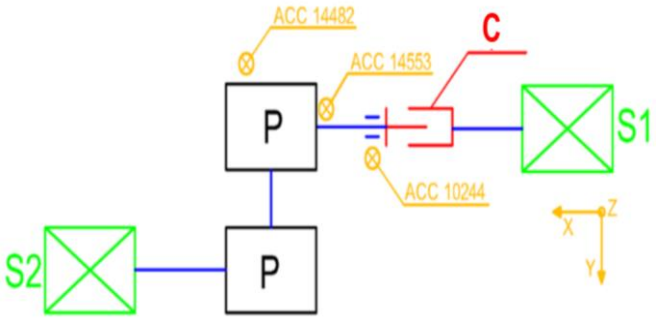

Fig. 10. Schematic diagram of the measuring sensor arrangement: S1 – electric drive motor, C – torsionally flexible clutch, P – gear transmissions (reducer and multiplier), S2 – electric braking motor (source: authors' contribution).

Prior to the main measurements, the temperature of the gear transmission and the highly flexible clutch was stabilised by operating the system for 1 hour under a torque-induced load of approx. 250 Nm and with a rotational speed of 1,480 rpm.

3. Test results and discussion

3.1. Determining the static characteristics of the highly flexible clutch (Stage 1)

Fig. 11 provides the torsion angle values measured for the operating member of the flexible clutch as a load torque function.

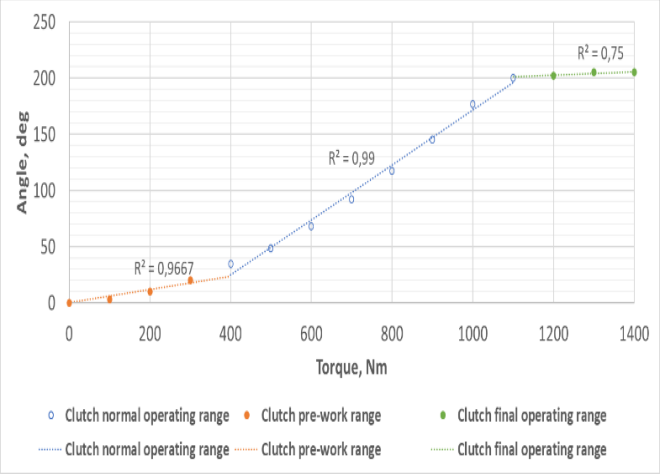

Fig. 11. Characteristics of the innovative flexible clutch examined in the studies (source: authors' contribution).

In the figure, one can distinguish between three phases of the clutch operation:

- initial operation phase, characterised by relatively small changes in the torsion angle on considerable changes in torque; this character of the clutch operation is attributable to the backlash between the springs, which is not eliminated until load is applied;
- main operation phase, characterised by a considerable angle change as a function of torsional moment;
- final operation phase, characterised by an inconsiderable change in torsion angle, which is only due to small elastic deformations of the shafts.

Based on the measurement results, a maximum torsion angle of the flexible clutch was determined at φ=205°. The static characteristics of the flexible clutch thus established made it also possible to determine the value of the load torque in Stages 2 and 3. The load variation values were pre-assumed in such a manner that they covered only the initial operation phase (T1=250±125Nm), partially the main and the initial operation phase (T2=500±250 Nm), and the entire main phase with fragments of the initial and final operation (T3=750±375 Nm). The load ranges envisaged in the studies have been illustrated in Fig. 12.

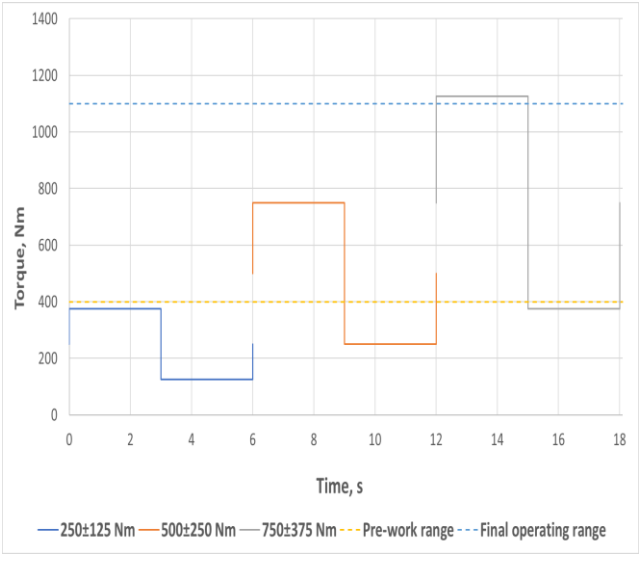

Fig. 12. Originally assumed torsional moment variation ranges against the boundary values of the initial and final operation phases (source: authors' contribution).

3.2. Determining torsional vibrations of the highly flexible clutch and the gear transmission housings (Stages 2 and 3)

In this section, results of the tests conducted in Stages 2 and 3

have been discussed jointly, which is due to the fact that – as the results have implied – the manner in which the transmission had been mounted exerted no effect on the values of the vibrations measured.

Fig. 13 illustrates the time courses of the signal of instantaneous changes in the angular velocity of the shaft driving the reduction gear, as recorded by a contactless method using the aforementioned Polytec RLV-5500 laser vibration meter. The instantaneous angular velocities of the drive shaft recorded when the clutch operation was blocked are marked in green colour, while the instantaneous angular velocities of the drive shaft recorded during the flexible operation of the clutch are shown in red.

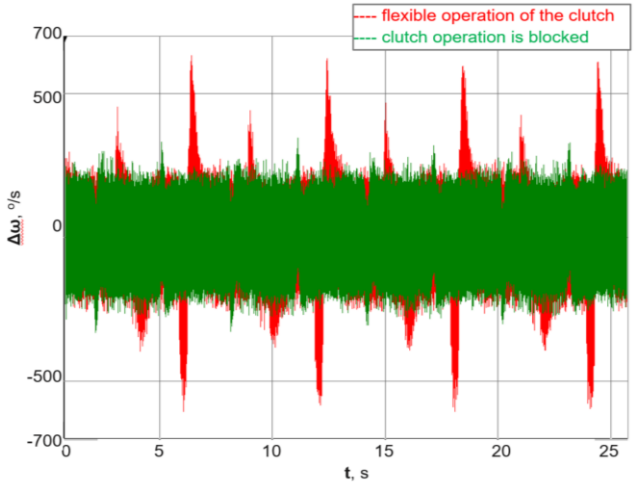

Fig. 13. Example of a time course of the signal of instantaneous torsional vibration velocity changes established for a torsional moment of 750 ±375 Nm with a square waveform (source: authors' contribution).

The instantaneous local maxima in the time course of the instantaneous variations in the signal of the drive shaft angular velocity (Fig. 13) marked in red result from the effect of a time-variable braking torque generated by the braking motor, which is transferred through the gear transmissions to the drive shaft and causes torsion of the flexible clutch members, but in this case, the dynamic overloads affecting the meshing are minimised by the flexibility of the innovative flexible clutch. On the other hand, where the clutch operation is blocked (green), the time-variable braking torque acts directly on the gear transmission meshing, causing their vibroactivity to increase, and on account of the action of the moment of inertia of the rotating gears and the drive shaft rotor, the load torque change does not cause such large instantaneous changes in the angular velocity of the shaft driving the flexible clutch, but instead, it exerts a considerable effect on the values of dynamic forces in the gear transmission's meshing and bearings as well as on the accelerations of the transmission housing vibrations.

The higher dynamic forces observed in the meshing in this operating mode contribute to faster degradation of both gears and bearings, and shorten the service life of this type of large multi-stage gear transmissions, the cost of which is relatively high.

The various aspects of shortened service life are inextricably linked with the problem of transport of such gear transmissions from the mine to the surface, where they are overhauled, and back underground. For this reason, extending their service life and ensuring reliable operation of these components is particularly important [3, 36].

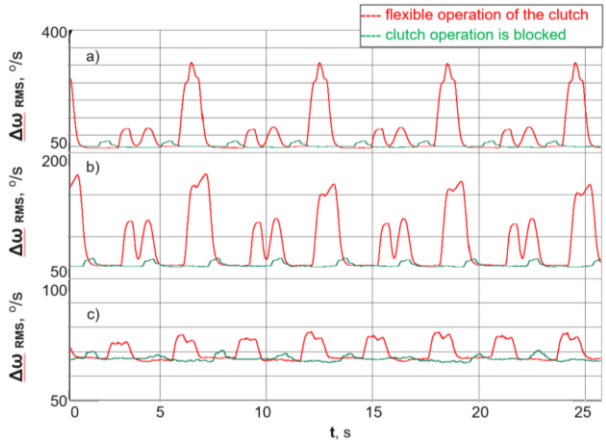

Fig. 14. RMS values of the instantaneous changes in the torsional vibration velocity, determined in a time window moved along the time axis, the system being loaded with a torque of square waveform: a) torque of 750 ±375 Nm, b) torque of 500 ±250 Nm, c) torque of 250 ±125 Nm (source: authors' contribution).

On account of the fact that, in the recorded signal of the instantaneous changes in the rotational speed of the reduction gear's input shaft, one can also observe signal components generated by the transmission meshing and bearings, which in this case may be treated as noise, in order to better demonstrate the effects of the clutch operation, filtering was applied, including determination of the RMS value of the vibration signal, calculated within a time window moved along the time axis with a period of 0.5 s (Fig. 14). Having calculated the RMS value, one can assess the energy of the vibration signal of the torsional vibration velocity.

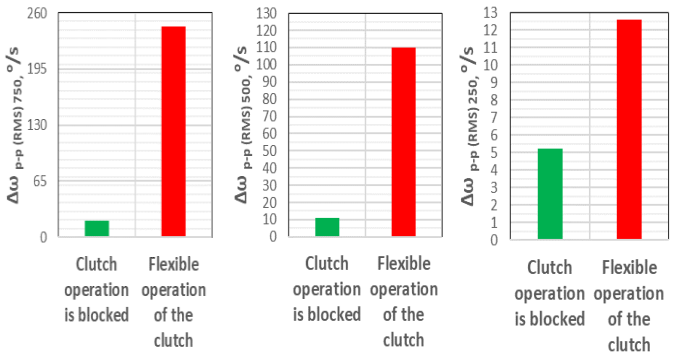

Fig. 15. Comparison of peak-to-peak values of the RMS signal of the instantaneous changes in the torsional vibration velocity, determined in a time window moved along the time axis, assuming that the system is loaded with a torque of square waveform: a) torque of 750 ±375 Nm, b) torque of 500 ±250 Nm, c) torque of 250 ±125 Nm.

Fig. 15 illustrates a comparison of the peak-to-peak values of the RMS signal of the instantaneous changes in the torsional vibration velocity, as determined in a time window moved along the time axis (shown in Fig. 14) for the rigid and flexible clutch operation. The significantly higher peak-to-peak values are indicative of the expected and correct operation of the clutch, resulting from its considerable torsional flexibility and the fact that it absorbs excess dynamic load due to the load torque changes.

There is a certain disadvantage to the RMS signal analysis, namely the absence of changes in the signal value for both the positive and the negative direction of the clutch torsion. This disadvantage does not apply to the mean value determined in a time window moved along the time axis, the period of which is also 0.5 s (Fig. 16).

Fig. 17 provides a comparison of the peak-to-peak values of the averaged signal of instantaneous changes in the torsional vibration velocity determined in a time window moved along the time axis (shown in Fig. 16) for both rigid and flexible operation of the clutch. Similarly to the RMS values, the peak-to-peak values being significantly higher imply that the clutch operates in the expected and correct manner, which results from its considerable torsional flexibility and the fact that it absorbs excess dynamic load due to the load torque changes.

Fig. 18 depicts the RMS values of the linear vibration accelerations recorded in direction x at the point marked as 14482, i.e. on the housing of the bearing of the shaft which transfers the highest torque in the gear transmission subject to analysis. Similarly to the instantaneous signals of the shaft angular velocity changes, these values (RMS) were determined in a time window moved along the time axis (period of 0.5 s).

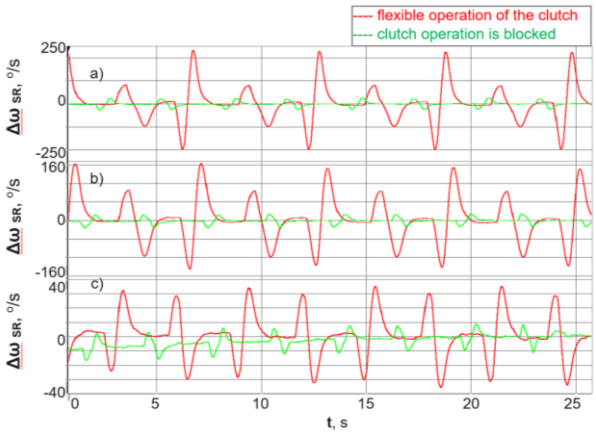

Fig. 16. Mean values of the instantaneous changes in the torsional vibration velocity, determined in a time window moved along the time axis, the system being loaded with a torque of square waveform: a) torque of 750 ±375 Nm, b) torque of 500 ±250 Nm, c) torque of 250 ±125 Nm (source: authors' contribution).

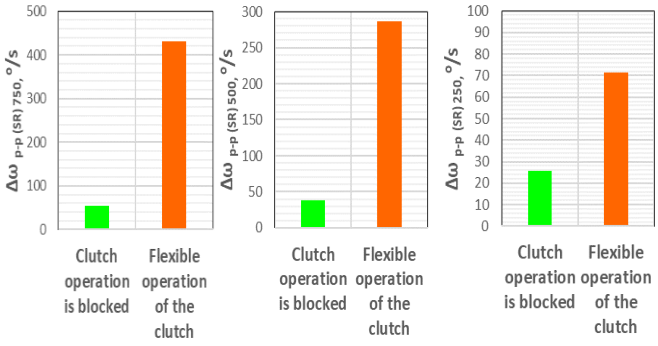

Fig. 17. Comparison of peak-to-peak values of an averaged signal of instantaneous changes in the torsional vibration velocity, the system being loaded with a torque of square waveform: a) torque of 750 ±375 Nm, b) torque of 500 ±250 Nm, c) torque of 250 ±125 Nm (source: authors' contribution).

Established in a similar manner, the RMS values of the vibration acceleration signals recorded at this point (14482), but in different directions (y and z), have been shown in Figures 19 and 20. What can be observed in Figures 18÷20 is that, in virtually every case, the RMS values determined in this manner are higher in the case of the rigid clutch operation, implying that the energy of the vibration acceleration signal is higher. The largest differences between the effects of the flexible clutch operation compared to its rigid operation mode can be observed in Figures 18 and 19 for the horizontal directions of the

vibration acceleration measurements, while smaller differences can be noticed in the vertical direction of the gravitational force effect.

Fig. 18. RMS values of the signal of the linear vibration accelerations established at point 14482, in direction x, in a time window moved along the time axis, the system being loaded with a torque of square waveform: a) torque of 750 ±375 Nm, b) torque of 500 ±250 Nm, c) torque of 250 ±125 Nm (source: authors' contribution).

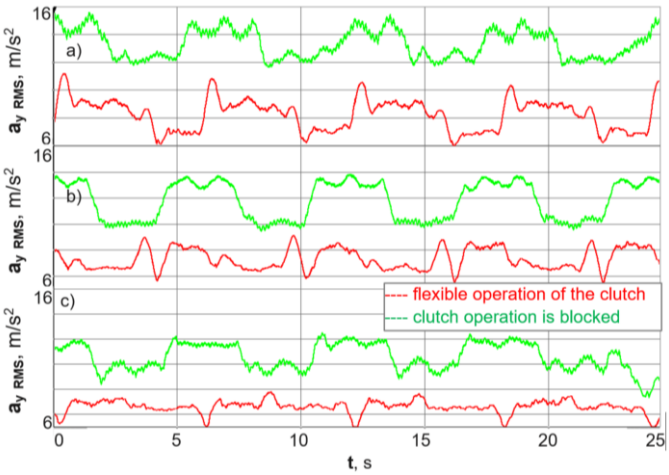

Fig. 19. RMS values of the signal of the linear vibration accelerations recorded at point 14482, in direction y, determined in a time window moved along the time axis, the system being loaded with a torque of square waveform: a) torque of 750 ±375 Nm, b) torque of 500 ±250 Nm, c) torque of 250 ±125 Nm (source: authors' contribution).

In order to better illustrate the results thus obtained, as provided in the said figures, RMS values were calculated for each of the cases analysed (Figure 21).

Having examined them, one can conclude that at the measuring point located on the bearing housing of the most heavily loaded shaft, for each of the measurement directions and each of the loads variable in time, the RMS values of linear vibration accelerations are higher in the case of the clutch operation being blocked.

A similar change trend in the cases of flexible and rigid operation of the clutch was also confirmed for most of the measurement directions and points located on the bearing housings, where the torques transferred by the shafts were lower, i.e. at the input shaft bearing housing in the reduction gear (Fig. 22) and the bearing housing at the clutch support (Fig. 23). Figure 24 provides a comparison of the RMS values of the linear vibration accelerations recorded in direction y at point 14553.

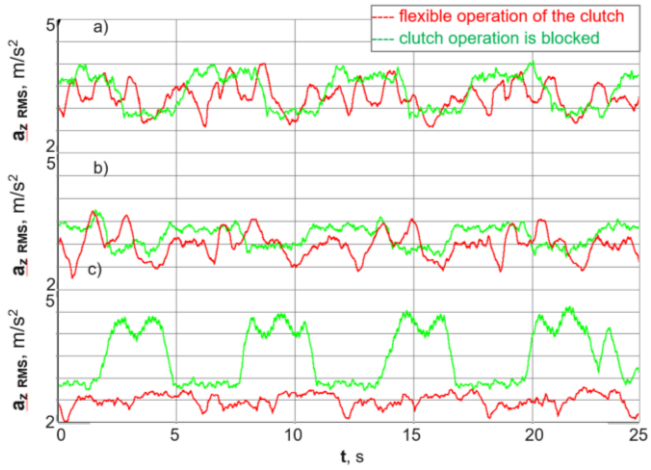

Fig. 20. RMS values of the signal of the linear vibration accelerations recorded at point 14482, in direction z, determined in a time window moved along the time axis, the system being loaded with a torque of square waveform: a) torque of 750 ±375 Nm, b) torque of 500 ±250 Nm, c) torque of 250 ±125 Nm (source: authors' contribution).

The values of the signals measured have been compared in Figures 25, 26, and 27. Having analysed them, one can conclude that a significant reduction of torsional vibrations can be obtained in the case where the clutch operation is blocked compared to the case where the flexible clutch is used in the power transmission system, but instead, in the cases analysed and where the flexible clutch was in use, a significant reduction of the linear vibrations recorded at the housings of the transmission bearings and of the clutch support bearing was obtained.

The only exception to this rule is the inconsiderable increase of 5% in the RMS values of the linear vibration accelerations recorded in direction y at point 14553 for the load torque of 750 ±375 Nm). The authors of this paper have found the foregoing

to be caused by the fact that, where the system is loaded according to the clutch characteristics provided in Fig. 11, with the maximum load torque value equal to 750 Nm + 375 Nm = 1,125 Nm, the clutch operation has already entered the final phase, which is characterised by moderately small changes in the torsional angle. In the cases of the other loads analysed: 500 ±250 Nm and 250 ±125 Nm, the reduction of the RMS values of vibration accelerations came to 24 and 52 per cent, respectively, which should be considered as considerable.

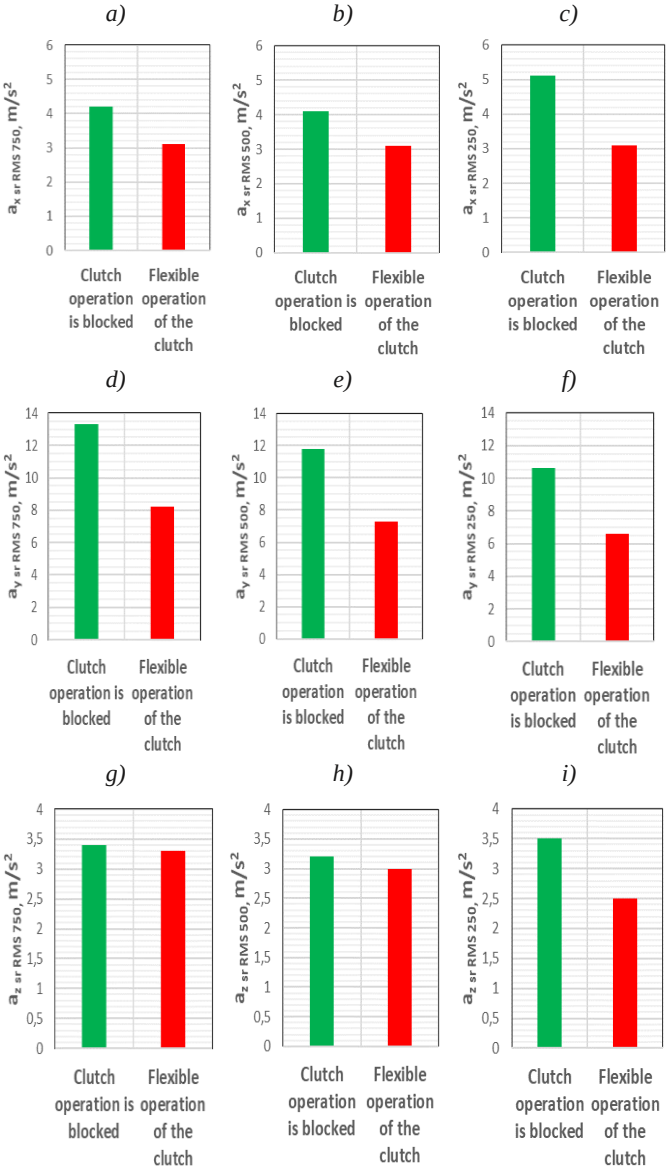

Fig. 21. Comparison of RMS values of linear vibration accelerations recorded at point 14482 in direction x: a) load of 750 ±375 Nm, b) load of 500 ±250 Nm, c) load of 250 ±125 Nm; in direction y: d) load of 750 ±375 Nm, e) load of 500 ±250 Nm, f) load of 250 ±125 Nm; in direction z: g) load of 750 ±375 Nm, h) load of 500 ±250 Nm, i) load of 250 ±125 Nm (source: authors' contribution).

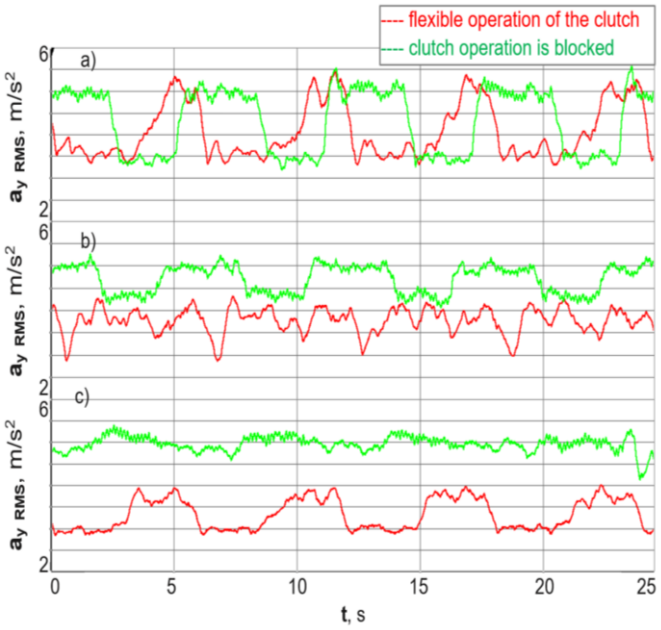

Fig. 22. RMS values of the signal of the linear vibration accelerations recorded at point 14553, in direction y, determined in a time window moved along the time axis, the system being loaded with a torque of square waveform: a) torque of 750 ±375 Nm, b) torque of 500 ±250 Nm, c) torque of 250 ±125 Nm (source: authors' contribution).

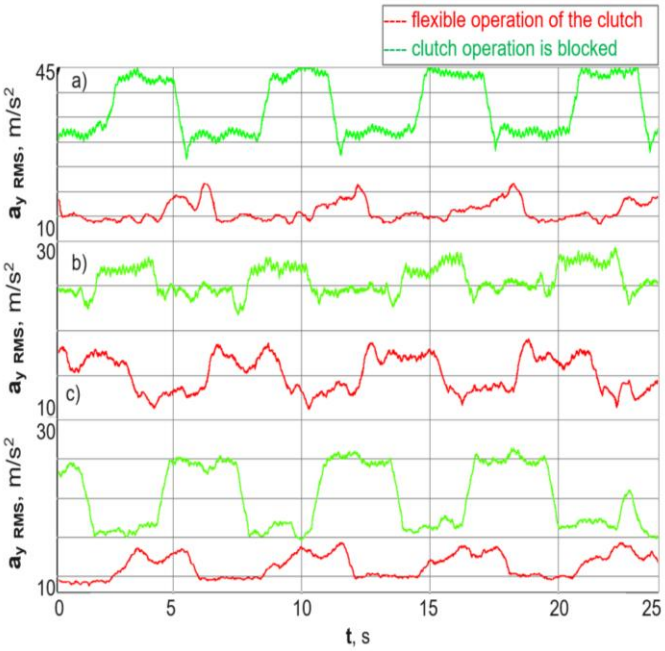

Fig. 23. RMS values of the signal of the linear vibration accelerations recorded at point 10244, in direction y, determined in a time window moved along the time axis, the system being loaded with a torque of square waveform: a) torque of 750 ±375 Nm, b) torque of 500 ±250 Nm, c) torque of 250 ±125 Nm (source: authors' contribution).

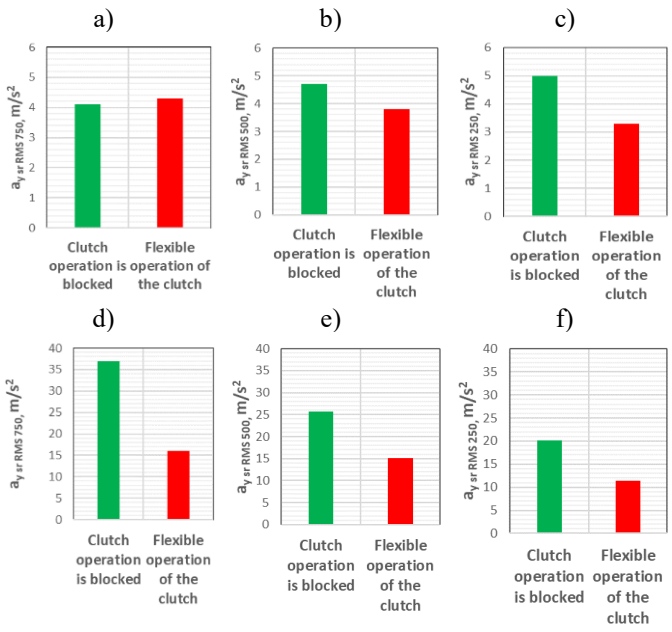

Fig. 24. Comparison of RMS values of linear vibration accelerations recorded in direction y, at point 14553: a) load of 750 ±375 Nm, b) load of 500 ±250 Nm, c) load of 250 ±125 Nm, and at point 10224: d) load of 750 ±375 Nm, e) load of 500 ±250 Nm, f) load of 250 ±125 Nm (source: authors' contribution).

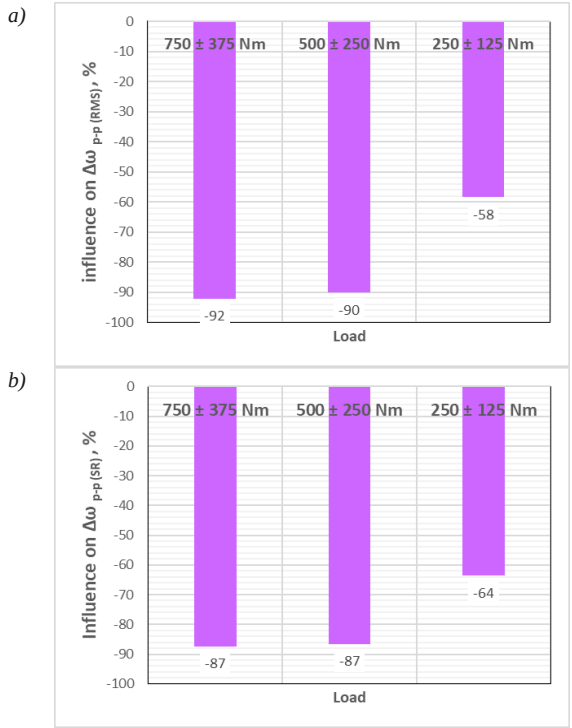

Fig. 25. Comparison of the effects attributable to using a blocked clutch and a flexible clutch on the reduction of: peak-to-peak values of the RMS signal of instantaneous torsional vibration velocity changes, determined in a time window moved along the time axis (a), peak-to-peak values of the averaged signal of instantaneous torsional vibration velocity changes (b) (source: authors' contribution).

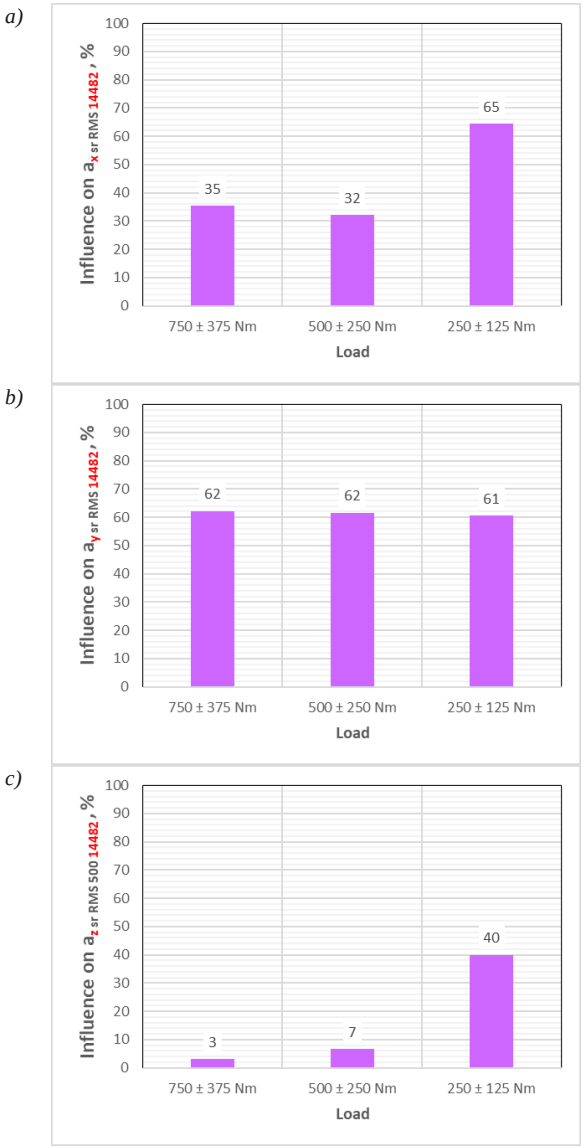

Fig. 26. Comparison of the effect attained by using a blocked clutch and a flexible clutch on the increase in the RMS values of linear vibration accelerations recorded at point 14482: a) in direction x, b) in direction y, c) in direction z (source: authors' contribution).

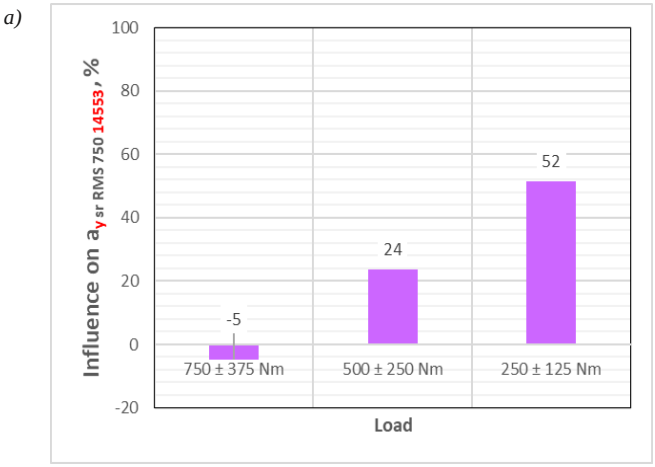

b)

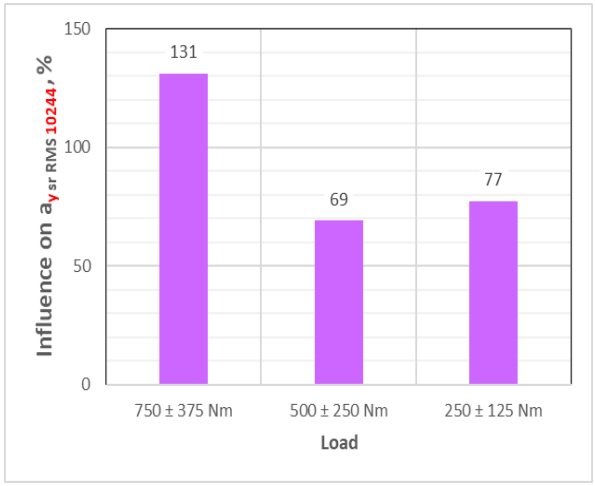

Fig. 27. Comparison of the effect attained by using a blocked clutch and a flexible clutch on the increase in the RMS values of linear vibration accelerations recorded in direction y: a) at point 14553: b) at point 10244 (source: authors' contribution).

3.3. Results of the durability tests of the highly flexible clutch components (Stage 4)

The purpose of Stage 4 was to verify if the flexible clutch components, and the bolt–nut system in particular, were resistant to repeated cycles of torsional moment variation. Fig. 28 shows the mating surfaces after approximately 1,200 cycles of such changes.

a) b)

Fig. 28. Surface of the bolt (a) and of the nut (b) following the durability tests.

Having analysed them, one can conclude that no significant surface damage had occurred. These observations were confirmed by the surface roughness measurements. One of the parameters controlled in the course of the durability tests was the flexible clutch surface temperature, based on which it was established that the motion of the mating surfaces against each other had a relatively small effect on heat generation (Fig. 29).

During the durability tests, the vibroactivity of the gear transmissions was monitored using the test rig equipment. They revealed no changes in the oscillatory condition of the transmission housings to have taken place between the start and end of the test.

Fig. 29. Thermograms of the flexible clutch subject to tests, as determined in the durability tests.

4. Conclusions

The following conclusions have been drawn on the basis of the tests and analyses discussed above.

1. One can distinguish between three phases of operation in the static characteristics of a highly flexible clutch: initial, main, and final, differing in terms of flexibility.
2. Having increased the flexibility of the metal clutch, one could observe the RMS values of the linear vibration accelerations recorded in direction y at point 10244 on the clutch support bearing housing to have dropped compared to the clutch operation being blocked, ranging between 69 and 131%, depending on the power transmission system load applied.
3. Once a highly flexible clutch had been used in the power transmission system, the RMS values of the signal of instantaneous changes of the angular velocity of the transmission drive shaft were found to have increased. Consequently, the linear vibrations recorded at the transmission bearing housings and at the clutch support bearing dropped significantly, i.e. by up to 65% and up to 131%, respectively, while in the cases of the load torques being as high as 500 ±250 Nm and 250 ±125 Nm, the RMS values of vibration accelerations were reduced by 24 and 52%, respectively. The only exception to this rule was the inconsiderable increase of 5% in the RMS values of the linear vibration accelerations recorded in direction y on the housing of the most heavily loaded transmission shaft when the braking torque came to 750 ±375 Nm. The foregoing can be explained in line with the pre-established static characteristics of the clutch as the consequence of having

limited its torsion on account of the fact that the maximum angle had been attained.

4. As a result of using the innovative flexible clutch in question, the aforementioned vibration reduction was recorded in many cases, i.e. for numerous measurement directions and points, and for high loads of 750 ±375 Nm, 500 ±250 Nm, and 250 ±125 Nm. This aspect is important for the very reason that, in the case of the rigid clutch operation, the higher dynamic forces acting in the transmission meshing, generated by load torque variable in time, are transferred from the meshing to the transmission shafts and further on to the bearings, and then, acting through the transmission bearings, they excite vibrations of the bearing housing, and thus of the entire transmission. What can be concluded on such a basis is that using the innovative flexible clutch in the power transmission system subject to the studies reduces the dynamic forces affecting the gear teeth as well as the bearings, thus extending the service life of the high-power mining gear transmissions in question, which are relatively cumbersome, costly, and difficult to replace or transport to the surface for repair purposes.
5. Based on the tests conducted in operating conditions, it was found that the durability of the flexibilising system (bolt and nut) was sufficient and that there were no thermal effects associated with the motion of the system components.

Acknowledgments

This research was developed under project POIR.04.01.04-00-0081/17 entitled “Develop innovative scraper conveyors with increased start-up flexibility and service life”, co-financed by the National Centre for Research and Development in Poland.

References

1. Angeles E, Kumral M. Optimal Inspection and Preventive Maintenance Scheduling of Mining Equipment. Journal of Failure Analysis and Prevention 2020; 20: 1408–1416, https://doi.org/10.1007/s11668-020-00949-z.
2. Andrych-Zalewska M, Chlopek Z, Pielecha J, Merkisz J. Investigation of exhaust emissions from the gasoline engine of a light duty vehicle in the Real Driving Emissions test. Eksploatacja i Niezawodność – Maintenance and Reliability. 2023;25(2). https://doi.org/10.17531/ein/165880.
3. Borucka A. Three-state Markov model of using transport means, Business Logistics in Modern Management, 2018;18:3-19
4. Butsch M. Hydraulische Verluste schnelllaufender Stirnradgetriebe, Dissertationen Universität Stuttgart 1989.
5. Can E, Bozca M. Optimising the Geometric Parameters of a Gear in a Tractor Transmission Under Constraints Using Kisssoft. Acta Mechanica et Automatica 2023, 17 (2): 145-159, https://doi.org/10.2478/ama-2023-0016.
6. Carranza Fernandez R, Tobie T, Collazo J. Increase wind gearbox power density by means of IGS (Improved Gear Surface). International Journal of Fatigue 2022; 159,, https://doi.org/10.1016/j.ijfatigue.2022.106789.
7. Cheng W, Wang S, Liu Y, Chen X, Nie Z, Xing J. Zhang R, Huang Q. A Novel Planetary Gearbox Fault Diagnosis Method for Nuclear Circulating Water Pump With Class Imbalance and Data Distribution Shift. IEEE Transactions on Instrumentation and Measurement 2023; 72: 1–13, https://doi.org/10.1109/tim.2023.3238752.
8. Clarke B P, Nicholas G, Hart E, Long H, Dwyer-Joyce R S. Loading on a wind turbine high-speed shaft gearbox bearing: Ultrasonic field measurements and predictions from a multi-body simulation. Tribology International 2023; 181, https://doi.org/10.1016/j.triboint.2023.108319.
9. Cocconcelli M, Agazzi A, Mucchi E, Dalpiaz G, Rubini R. Dynamic analysis of coupling elements in IC engine test rigs. In Proceedings of the ISMA2014-USD2014 Conference, Leuven, Belgium, 15–17 September 2014: 1005–1018.
10. da Silva Tuckmantel F W, Cavalca K L. Vibration signatures of a rotor-coupling-bearing system under angular misalign-ment. Mechanism and Machin Theory 2019; 133: 559–583, https://doi.org/10.1016/j.mechmachtheory.2018.12.014.
11. Dao P B. On Cointegration Analysis for Condition Monitoring and Fault Detection of Wind Turbines Using SCADA Data. Energies 2023; 16 (5), https://doi.org/10.3390/en16052352.
12. Dhote N D, Khond M P. Condition Monitoring Approach for Wear Recognition in Gear Pump. Journal of Failure Analysis and Prevention 2022; 22(4): 1558-1565, https://doi.org/10.1007/s11668-022-01448-z.

13. Dick A: Untersuchungen zu den Leerlaufverlusten eines einspritzgeschmierten Stirnradgetriebes, Dissertationen Universität Stuttgart 1989.
14. Döbereiner R.: Tragfähigkeit von Hochverzahnungen geringer Schwingungsanregung. Praca doktorska TU München 1998.
15. Dolipski M, Sobota P. Porównanie rozruchu przenośnika zgrzebłowego ze sprzęgłami hydrokinetycznymi i podatnymi. Przegląd Górniczy 1992: 1–254.
16. Dolipski M. Ugleichmaessige Belastung von Antriebssystemen in kettengetriebenen Betriebsmitteln mit Kopf- und Heckantrieb. Trier, In Proceedings of the 5. Ingenieurtag am Fachbereich Maschinenban der FH Trier.
17. Drwięga A, Skoć A. Badanie Charakterystyk Dynamicznych Sprzęgła Wielopłytkowego Zintegrowanego z Przekładnią Zębatą Obiegową Napędu Przenośników Górniczych. Gliwice, Wydawnictwo Komag: 2006.
18. Durczak K, Selech J, Ekielski A, Żelaziński T, Waleński M, Witaszek K. Using the Kaplan–Meier Estimator to Assess the Reliability of Agricultural Machinery. Agronomy, 2022, 12, 1364, https://doi.org/10.3390/agronomy12061364.
19. Feng K, Ji J C, Ni Q, Yun H, Zheng J, Liu Z. A novel vibration indicator to monitor gear natural fatigue pitting propagation. Structural Health Monitoring 2023; 0(0), https://doi.org/10.1177/14759217221142622.
20. Feng K, Ni Q, Beer M, Du H, Li C. A novel similarity-based status characterization methodology for gear surface wear propagation monitoring. Tribology International 2022; 174, https://doi.org/10.1016/j.triboint.2022.107765.
21. Filipowicz K. Dwukierunkowe Metalowe Sprzęgła Podatne Skrętnie. Gliwice, Wydawnictwo Politechniki Śląskiej: 2011.
22. Fill-controlled Fluid Couplings, broszura firmy Voith TurboGmbH & Co. KG, Crailsheim 2007.
23. Gao Y, Liu X, Xiang J. Fault Detection in Gears Using Fault Samples Enlarged by a Combination of Numerical Simulation and a Generative Adversarial Network. IEEE/ASME Transactions on Mechatronics 2022; 27 (5): 3798-3805. https://doi.org/10.1109/TMECH.2021.3132459
24. Gauder D, Gölz J, Jung N, Lanza G. Development of an adaptive quality control loop in micro-production using machine learning, analytical gear simulation, and inline focus variation metrology for zero defect manufacturing. Computers in Industry 2023; 144, https://doi.org/10.1016/j.compind.2023.103854.
25. Gerber H. Innere dynamische Zusatzkräkte bei Stirnradgetrieben – Modelbildung, innere Anregung und Dämpfung. Praca doktorska TU München 1984.
26. Grega R, Krajnak J, Žuľová L, Kačír M, Kaššay P, Urbanský M. Innovative Solution of Torsional Vibration Reduction by Application of Pneumatic Tuner in Shipping Piston Devices. Journal of Marine Science and Engineering 2023; 11(2), 261, https://doi.org/10.3390/jmse11020261.
27. Hawk J A, Wilson R D. Tribology of Earthmoving, Mining, and Minerals Processing. In Modern Tribology Handbook, CRC Press LLC: 2001. https://doi.org/10.1201/9780849377877.ch35
28. Höhn B R, Oster P, Döbereiner R. Load Capacity of High Ratio Gears Comparision of Theoretical Calculation and Experimatal Test Results. VDI – Berichte 2002; 1665.
29. Homišin J, Kaššay P, Urbanský M, Puškár M, Grega R, Krajňák J. Electronic Constant Twist Angle Control System Suitable for Torsional Vibration Tuning of Propulsion Systems. Journal of Marine Science and Engineering 2020; 8 (721), https://doi.org/10.3390/jmse8090721.
30. Inturi V, Balaji S V, Gyanam P, Pragada B P V, Geetha Rajasekharan S, Pakrashi V. An integrated condition monitoring scheme for health state identification of a multi-stage gearbox through Hurst exponent estimates. Structural Health Monitoring 2023; 22(1): 730-745, https://doi.org/10.1177/14759217221092828.
31. Juzek, M. Analysis of the impact of non-parallelism of shafts' axes on the contact area of cooperating teeth and gearbox's components vibrations. Scientific Journal of Silesian University of Technology. Series Transport 2019; 104: 37-45. https://doi.org/10.20858/sjsutst.2019.104.4.
32. Kowal A. Sprzęgło Mechaniczne. Patent No. PL 190945 B1, 28 February 2006; r. WUP 02/06.
33. Kowal A. Sprzęgło Mechaniczne. Patent No. PL 191092 B1, 31 March 2006; r. WUP 03/06.
34. Kowal A, Filipowicz K. The construction of metal flexible torsional coupling. Transport Problems 2007; 2: 73–80.
35. Kozłowski, E., Borucka, A., Liu, Y., Mazurkiewicz, D. Conveyor Belts Joints Remaining Life Time Forecasting with the Use of Monitoring Data and Mathematical Modelling. Innovations in Mechatronics Engineering 2021: https://doi.org/10.1007/978-3-030-79168-1_5
36. Kozłowski E, Borucka A, Oleszczuk P, Jałowiec T. Evaluation of the maintenance system readiness using the semi-Markov model taking

into account hidden factors. Eksploatacja i Niezawodność – Maintenance and Reliability. 2023;25(4). https://doi.org/10.17531/ein/172857
37. Li X, Zhang W, Yang J, Wang B. Compensation of axial geometric errors in cycloidal gear form grinding. Journal of Manufacturing Processes 2022; 71: 110-126. https://doi.org/10.1155/2022/4804498
38. Li Y, Du X, Wang X, Si S. Industrial gearbox fault diagnosis based on multi-scale convolutional neural networks and thermal imaging. ISA Transactions 2022; 129: 309-320, https://doi.org/10.1016/j.isatra.2022.02.048.
39. Lin H, Oswald F B, Townsend D P. Computer-Aided of High-Contact-Ratio Gears for Minimum Dynamic Load and Stress. Journal of Mechanical Design 1993; 115 (1), https://doi.org/10.1115/1.2919315.
40. Łazarz B, Perun G. Determining the technical state of a combustion engine with the use of vibroacoustic signals. Zeszyty Naukowe 2016; 4: 117-124.
41. Michalczewski R, Kalbarczyk M, Slomka Z, Sowa S, Łuszcz M, Osuch-Słomka E, Maldonado-Cortés D, Liu L, Antonov M, Hussainova I. The wear of PVD coated elements in oscillation motionat high temperature. Proceedings of the Estonian Academy of Sciences 2021, 70: 500–507.
42. Michnej M, Młynarski S, Pilch R, Sikora W, Smolnik M, Drożyner P. Physical and reliability aspects of high-pressure ammonia water pipeline failures. Eksploatacja i Niezawodnosc – Maintenance and Reliability 2022, 24, 4, http://doi.org/10.17531/ein.2022.4.13.
43. Kuczaj M, Wieczorek A N, Konieczny Ł, Burdzik R, Wojnar G, Filipowicz K, Głuszek G. Research on Vibroactivity of Toothed Gears with Highly Flexible Metal Clutch under Variable Load Conditions. Sensors 2023; 23(1), 287, https://doi.org/10.3390/s23010287.
44. Markusik S. Sprzęgła mechaniczne. Warszawa, Wydawnictwa Naukowo-Techniczne: 1979.
45. Maurer J. Lastunabhängige Verzahnungsverluste schnellaufender Stirnradgetriebe, Dissertationen Universität Stuttgart 1994.
46. Mauz W. Hydraulische Verluste von Stirnradgetrieben bei Umfangsgeschwindigkeiten bis 60 m/s, Dissertationen Universität Stuttgart 1987.
47. Möllers W. Parametererregte Schwingungen in einstufigen Zylinderradgetrieben. Einfluss von Verzahnungsabweichungen und Verzahnungssteifigkeitsspektren. Praca doktorska. RWTH Aachen 1982.
48. Salje H. Konstruktive Geräuschminderungsmassnahmen durch gezielte Profilkorrektu-ren und Hochverzahnungen. Forschungsvorhaben Nr. 98/I, Frankfurt 1985.
49. Salje H. Tragfähigkeits- und Geräuschuntersuchungen an Hochverzahnungen - Ab-schlussbericht. Forschungsvorhaben Nr. 98/II, Frankfurt 1987.
50. Shao W, Yi M, Tang J, Sun S. Prediction and Minimization of the Heat Treatment Induced Distortion in 8620H Steel Gear: Simulation and Experimental Verification. Chinese Journal of Mechanical Engineering (English Edition) 2022; 35(1), https://doi.org/10.1186/s10033-022-00802-4.
51. Shi Z, Zhu Z. Case study: Wear analysis of the middle plate of a heavy-load scraper conveyor chute under a range of operating conditions. Wear 2017; 380–381: 36–41, https://doi.org/10.1016/j.wear.2017.03.005.
52. Shi C Z, Parker R G. Modal structure of centrifugal pendulum vibration absorber systems with multiple cyclically symmetric groups of absorbers. Journal of Sound and Vibration 2013; 332 (18): 4339–4353, https://doi.org/10.1016/j.jsv.2013.03.009.
53. Skołek E, Wasiak K, Świątnicki W A. Structure and properties of the carburised surface layer on 35CrSiMn5-5-4 steel after nanostructurization treatment. Materials and Technology 2015; 49, https://doi.org/10.17222/mit.2014.255.
54. Sobota P. Identyfikacja i określenie możliwości redukcji przeciążeń zespołów napędowych w przenośnikach ścianowych. BW-592/RG-2/98/T-9, Gliwice 1998 (unpublished work).
55. Strasser D. Einfluss des Zahnflanken- und Zahnkopfspieles auf die Leerlaufverlustleistung von Zahnradgetrieben, Dissertationen Ruhr-Universität Bochum 2005.
56. Suchoń J. Górnicze przenośniki zgrzebłowe. Gliwice, Budowa i zastosowanie. Instytut Techniki Górniczej KOMAG: 2012.
57. Suchoń J. Górnicze przenośniki zgrzebłowe. Gliwice, Teoria, badania i eksploatacja. Instytut Techniki Górniczej KOMAG: 2012.
58. Timokhina I B, Beladi H, Xiong X Y, Adachi Y, Hodgson P D. Nanoscale microstructural characterization of a nanobainitic steel. Acta Materialia 2011; 59: 5511–5522. https://doi.org/10.1016/j.actamat.2011.05.024.
59. Tobie T, Hippenstiel F, Mohrbacher H. Optimizing gear performance by alloy modification of carburizing steels. Metals 2017; 7, https://doi.org/10.3390/met7100415.

60. Tylczak J H. Abrasive wear. In ASM Handbook—Friction, Lubrication, and Wear Technology 1992: 184–190.
61. Ulbrich D, Selech J, Kowalczyk J, Jóźwiak J, Durczak K, Gil L, Pieniak D, Paczkowska M, Przystupa K. Reliability Analysis for Unrepairable Automotive Components. Materials 2021, 14, 7014, https://doi.org/10.3390/ma14227014.
62. Walter P. Untersuchungen zur Tauchschmierung von Stirnrädern bei Umfangsgeschwindigkeiten bis 60 m/s, Dissertationen Universität Stuttgart 1982.
63. Wang, H, Li Z. Safety management of coal mining process. In IOP Conference Series: Earth and Environmental Science, IOP Publishing 2020; 598, https//doi:10.1088/1755-1315/598/1/012005.
64. Weck M. Moderne Leistunggetriebe. Springer-Verlag, Berlin, Heidelberg, New York, London, Paris, Tokyo 1995.
65. Wieczorek A N, Konieczny Ł, Burdzik R, Wojnar G, Filipowicz K, Kuczaj M. A Complex Vibration Analysis of a Drive System Equipped with an Innovative Prototype of a Flexible Torsion Clutch as an Element of Pre-Implementation Testing. Sensors 2022; 22(6), 2183, https://doi.org/10.3390/s22062183.
66. Wieczorek A N. Analysis of the possibility of integrating a mining right-angle planetary gearbox with technical diagnostics systems. Scientific Journal of Silesian University of Technology. Series Transport 2016; 93: 149-163, https://doi.org/10.20858/sjsutst.2016.93.16.
67. Wieczorek N, Polis W. Operation-oriented method for testing the abrasive wear of mining chain wheels in the conditions of the combined action of destructive factors. Management Systems in Production Engineering, 2015, 3, 19, https://doi.org/10.12914/MSPE-12-03-2015.
68. Wojnar G, Burdzik R, Wieczorek A N, Konieczny Ł. Multidimensional Data Interpretation of Vibration Signals Registered in Different Locations for System Condition Monitoring of a Three-Stage Gear Transmission Operating under Difficult Conditions. Sensors 2021; 21(23), 7808, https://doi.org/10.3390/s21237808.
69. Wu D, Yan P, Guo Y, Zhou H, Chen J. A gear machining error prediction method based on adaptive Gaussian mixture regression considering stochastic disturbance. Journal of Intelligent Manufacturing 2022; 33 (8): 2321-2339, https://doi.org/10.1007/s10845-021-01791-2.
70. Xia R, Li B, Wang X, Yang Z, Liu L. Screening the Main Factors Affecting the Wear of the Scraper Conveyor Chute Using the Plackett–Burman Method. Hindawi Mathematical Problems in Engineering 2019, 2019: 1–11, https://doi.org/10.1155/2019/1204091.
71. Yi, Y.; Qin, D.; Liu, C. Investigation of electromechanical coupling vibration characteristics of an electric drive multistage gear system. Mechanism and Machine Theory 2018; 121: 446–459, https://doi.org/10.1016/j.mechmachtheory.2017.11.011.
72. Zum Gahr K H. Microstructure and Wear of Materials. Tribology series. Amsterdam, Elsevier: 1987.